

Utility Optimal Scheduling with a Slow Time-Scale Index-Bias for Achieving Rate Guarantees in Cellular Networks

Anurag Kumar
ECE Department
Indian Institute of Science
Bengaluru, India
anurag@iisc.ac.in

Rajesh Sundaesan
ECE Department
Indian Institute of Science
Bengaluru, India
rajeshs@iisc.ac.in

Abstract—One of the requirements of *network slicing* in 5G networks is RAN (radio access network) scheduling *with rate guarantees*. We study a three-time-scale algorithm for maximum sum utility scheduling, with minimum rate constraints. As usual, the scheduler computes an index for each UE in each slot, and schedules the UE with the maximum index. This is at the fastest, natural time-scale of channel fading. The next time-scale is of the exponentially weighted moving average (EWMA) rate update. The slowest time scale in our algorithm is an “index-bias” update by a stochastic approximation algorithm, with a step-size smaller than the EWMA. The index-biases are related to Lagrange multipliers, and bias the slot indices of the UEs with rate guarantees, promoting their more frequent scheduling. We obtain a pair of coupled ordinary differential equations (o.d.e.) such that the unique stable points of the two o.d.e.s are the primal and dual solutions of the constrained utility optimization problem. The UE rate and index-bias iterations track the asymptotic behaviour of the o.d.e. system for small step-sizes of the two slower time-scale iterations. Simulations show that, by running the index-bias iteration at a slower time-scale than the EWMA iteration and using the EWMA throughput itself in the index-bias update, the UE rates stabilize close to the optimum operating point on the rate region boundary, and the index-biases have small fluctuations around the optimum Lagrange multipliers. We compare our results with a prior two-time-scale algorithm and show improved performance.

I. INTRODUCTION

An important functionality that has been planned for 5G cellular networks, and beyond, is that of *network slicing* (see, for example, [4]). A “slice” in a 5G network would be a virtual subnetwork extending from the point of Internet access, all the way through the transport and core, up to and including the radio access network (RAN), configured to provide some desired services to the user connections carried on that slice. One such service could be that the connections carried by the slice are guaranteed a minimum average aggregate throughput. With the backhaul comprising high-speed optical network links, the bottleneck in the provision of such rate guarantees would be the RAN. In this paper, we are concerned with RAN schedulers that can also provide rate guarantees.

We consider the downlink of a single base station (BS) with several associated UEs (user equipments). The radio access is

time slotted. In each slot, the BS uses the information about the rates that can be allotted to the UEs in the slot, along with the average throughputs achieved thus far by the UEs, to dynamically determine the rates to be allotted to the UEs in the current slot. The popular approach is based on a dynamic allocation scheme that, in the long run, results in average UE throughputs that maximize the total utility over the UEs, where each UE’s utility is a concave, increasing function of its throughput (see, for example, [7]). Network slicing motivates sum utility optimal scheduling with minimum rate guarantees. We consider the provision of individual minimum rate guarantees to some of the UEs, assuming that the guarantees are feasible, and provide an extension of the usual dynamic scheduling algorithm such that resulting average throughputs respect the desired minimum rate guarantees.

A. Related Literature

After the original proportional fair scheduling algorithm was introduced (using log of throughput as the utility), there was a series of papers that provided a deeper understanding, and proofs of convergence of generalizations of the algorithm to other concave nondecreasing utility functions; see [2], [7], [11]; see also [10] for a recent treatment of the problem. The approach has been to consider a sequence of instances of the algorithm with reducing weights for the EWMA (exponentially weighted moving average) throughput calculation (i.e., increasing averaging window). It is shown, then, by fluid limit arguments, that the EWMA throughputs track a certain ordinary differential equation (o.d.e.), whose unique stable point is the solution of the utility optimization over a rate region that is the average of the slot-wise rate regions, the average being taken over the stationary probability distribution of the joint channel state Markov chain.

After the introduction of the network slicing concept in the 5G cellular network standards, there has been interest in scheduling with rate guarantees. An important precursor to our work reported in this paper is the work by Mandelli et al. [9], where the authors modify the calculation of certain indices used in the classical scheduler by an additive *bias*. This bias

is updated by an additive correction obtained by comparing the *rate allocated in the current slot* against the minimum guaranteed rate. The authors, essentially, extend an algorithm provided in [12, Section 6], and utilize the convergence proof of [11]. The EWMA update and the bias update have a common time-scale. Simulation results are presented that show that the network utility improves as compared to other proposals for scheduling with rate guarantees.

B. Contributions and Outline

In our work, we have considered dynamic rate allocation algorithms for the minimum rate constrained utility optimization problem, assuming that the problem is feasible. It is easy to see (Section III-A) that the index-biases that promote the rate guarantees are the Lagrange multipliers in the optimal solution of the utility maximization problem. We use a stochastic approximation (SA) algorithm to update the Lagrange multipliers *based on the EWMA rates*, rather than the allocated rates in a slot (see Section III-B). The step size in the SA update is smaller than the averaging weight used in the EWMA calculation. Thus, in addition to the natural time-scale at which the channel is varying slot-to-slot, there are two, successively slower, time-scales, namely, the EWMA update time-scale for the throughputs and the SA update time-scale for the Lagrange multipliers.

In comparison with the algorithm proposed in [9], we find that our algorithm provides (i) accurate convergence to the desired operating throughputs with rate guarantees, and (ii) smooth behaviour of the index-biases which are approximations to the Lagrange multipliers. The two step-sizes (of the two SA iterations) can predictably control the rate of convergence and accuracy (see Section V). Accurate estimates of the Lagrange multipliers are useful to the network operator for the purposes of pricing and admission control. Further, the standard or user requirements may specify the throughput averaging time-scale, in which case, a separate time-scale for the index-bias update gives the operator the flexibility to ensure that the Lagrange multipliers are estimated accurately. See, for example, [1, Table 5.7.4-1] where the averaging window for guaranteed rate services is given as 2000 ms.

In Section IV, under certain conditions, we show that the UE throughputs and the index-biases track the trajectories of two coupled o.d.e.s, whose unique stable point is the optimal primal-dual solution of the minimum rate constrained utility optimization problem.

II. SYSTEM MODEL, NOTATION, & PROBLEM DEFINITION

There is a single gNB (generically a Base Station (BS)). The slots are indexed by $k, k \geq 0$. Vectors are typeset in bold font, and are viewed as column vectors.

- M : The number of UEs, indexed by $i, 1 \leq i \leq M$
- \mathcal{S} : The set of joint channel states for the UEs; in a slot, the state $s \in \mathcal{S}$ is known to the scheduler, and fixes the number of bits each UE can transmit in the slot

$S(k)$: For $k \geq 0$, is the joint channel state process, assumed to be a Markov chain on \mathcal{S} , whose realization $s(k)$ in a slot k is known to the scheduler

$P(\cdot|s)$: Transition probability kernel of the channel state process Markov chain $\{S_k, k \geq 0\}$

π_s : ($s \in \mathcal{S}$) is the stationary probability of the channel state process $\{S_k, k \geq 0\}$

\mathcal{R}_s : $\subset \mathbb{R}_+^M$; the joint rate region for the M UEs in a slot when the channel state in the slot is $s \in \mathcal{S}$; for every $s \in \mathcal{S}$, \mathcal{R}_s is convex and coordinate convex¹

$\overline{\mathcal{R}}_{\cdot|s}$: $\subset \mathbb{R}_+^M$; the rate region of the vector of average rates over a slot, given that the previous state is s ; clearly, $\overline{\mathcal{R}}_{\cdot|s} = \sum_{s' \in \mathcal{S}} P(s'|s) \mathcal{R}_{s'}$; by the assumptions on $\mathcal{R}_{s'}$, $\overline{\mathcal{R}}_{\cdot|s}$ is convex and coordinate convex

$\overline{\mathcal{R}}$: $\subset \mathbb{R}_+^M$; the rate region of the vector of average rates over the slots; clearly, $\overline{\mathcal{R}} = \sum_{s \in \mathcal{S}} \pi_s \mathcal{R}_s$, and $\overline{\mathcal{R}}$ is convex and coordinate convex

$\hat{\mathcal{R}}$: $([0, \hat{r}] \times [0, \hat{r}] \times \cdots \times [0, \hat{r}]) \subset \mathbb{R}_+^M$ where \hat{r} is the maximum possible bit rate at which a gNB can transmit to a UE; $\mathcal{R}_s, \overline{\mathcal{R}}_{\cdot|s}, \overline{\mathcal{R}}$ are all subsets of $\hat{\mathcal{R}}$

$U(\mathbf{r})$: The utility of the rate vector $\mathbf{r} \in \mathcal{R}$; $U(\mathbf{r})$ is strictly concave, coordinate-wise nondecreasing over $\overline{\mathcal{R}}$, and continuously differentiable; typically, $U(\mathbf{r}) = \sum_{i=1}^M U_i(r_i)$, with $U_i(\cdot)$ strictly concave, nondecreasing, and continuously differentiable

$\theta_i(k)$: The EWMA throughput of UE $_i$ at the beginning of slot k ; $\boldsymbol{\theta}(k) = (\theta_1(k), \theta_2(k), \cdots, \theta_M(k))^T$, the column vector of all the EWMA throughputs at the beginning of slot k

$r_i(k)$: The rate obtained by UE $_i$ in slot k ; $\mathbf{r}(k) = (r_1(k), r_2(k), \cdots, r_M(k))^T$, the column vector of rates obtained by all the UEs in slot k

$\theta_{i,\min}$: the rate guarantee for UE $_i$, possibly equal to 0; $\boldsymbol{\theta}_{\min}$ the vector of rate guarantees

$\nu_i(k)$: the nonnegative *index bias* used for enforcing the rate guarantee for UE $_i$
 $\boldsymbol{\nu}(k) = (\nu_1(k), \nu_2(k), \cdots, \nu_M(k))^T$

The *optimization problem* we consider in this work is:

$$\max U(\mathbf{r}) \text{ subject to } \mathbf{r} \in \overline{\mathcal{R}} \cap \{\mathbf{r} \in \mathbb{R}_+^M : \mathbf{r} \geq \boldsymbol{\theta}_{\min}\} \quad (1)$$

Assuming that Problem (1) is feasible, due to the strict concavity of $U(\cdot)$ and the convexity of the rate region $\overline{\mathcal{R}}$, we have a unique vector of optimum rates $\boldsymbol{\theta}^* \in \overline{\mathcal{R}}$.

The *scheduling problem* is: in a slot, given the state $s(k)$ and the EWMA throughputs $\boldsymbol{\theta}(k)$, determine a rate assignment $\mathbf{r}(k)$ so that the vector of EWMA rates eventually gets close (in some sense) to $\boldsymbol{\theta}^*$.

III. SCHEDULING WITH RATE GUARANTEES

A. Motivation for the algorithm

Denoting by $co\{\cdot\}$ the convex hull of a set, consider the special case where, for each $s \in \mathcal{S}$, $\mathcal{R}_s = co\{\mathbf{r}_{s,i}, 1 \leq i \leq M\}$, where $\mathbf{r}_{s,i} = (0, \cdots, 0, r_{s,i}, 0, \cdots, 0)$, with $r_{s,i} \geq 0$, at

¹A set is coordinate convex if $\mathbf{r} \in \mathcal{R}_s$ implies $\{\mathbf{x} : \mathbf{0} \leq \mathbf{x} \leq \mathbf{r}\} \subset \mathcal{R}_s$.

the i^{th} position, the rate UE_i gets if scheduled alone when the channel state is s . This special case corresponds to the situation in which, in each slot, any one UE is scheduled.

For a scheduling algorithm, for an $s \in \mathcal{S}$ and $1 \leq i \leq M$, let $x_{s,i}$ be the fraction of slots in which UE_i is scheduled when the channel state is s . Here, for an $s \in \mathcal{S}$, $x_{s,i} \geq 0$, $1 \leq i \leq M$, and $\sum_{i=1}^M x_{s,i} \leq 1$. Clearly, any $\mathbf{r} \in \mathcal{R}_s$ can be achieved by such time-sharing over slots when the channel state is s .

The optimization problem (1) becomes

$$\begin{aligned} \max \quad & \sum_{i=1}^M U_i(\theta_i) \\ \theta_i \quad & = \sum_{s \in \mathcal{S}} \pi_s x_{s,i} r_{s,i} \\ \theta_i \quad & \geq \theta_{i,\min} \end{aligned}$$

for all $s \in \mathcal{S}$, $\sum_{i=1}^M x_{s,i} \leq 1$, and $x_{s,i} \geq 0$ (2)

Since the $U_i(\cdot)$ are strictly concave, we are optimizing a concave function over linear constraints. Hence, the Karush-Kuhn-Tucker (KKT) conditions are necessary and sufficient.

For $s \in \mathcal{S}$ and $1 \leq i \leq M$, $\nu_i \geq 0$, $\lambda_s \geq 0$ and $\eta_{s,i} \geq 0$, we have the Lagrangian function

$$\begin{aligned} L(\mathbf{x}, \boldsymbol{\nu}, \boldsymbol{\lambda}, \boldsymbol{\eta}) := & \sum_{i=1}^M \left(U_i \left(\sum_{s \in \mathcal{S}} \pi_s x_{s,i} r_{s,i} \right) + \nu_i \left(\sum_{s \in \mathcal{S}} \pi_s x_{s,i} r_{s,i} - \theta_{i,\min} \right) \right) \\ & + \sum_{s \in \mathcal{S}} \lambda_s \left(1 - \sum_{i=1}^M x_{s,i} \right) + \sum_{s \in \mathcal{S}} \sum_{i=1}^M \eta_{s,i} x_{s,i} \end{aligned}$$

We need a KKT point $(\mathbf{x}^*, \boldsymbol{\nu}^*, \boldsymbol{\lambda}^*, \boldsymbol{\eta}^*)$ that satisfies (writing $\theta_i^* = \sum_{s \in \mathcal{S}} \pi_s x_{s,i}^* r_{s,i}$), for every $s \in \mathcal{S}$ and $1 \leq i \leq M$:

$$\begin{aligned} \frac{d}{d\theta_i} U_i(\theta_i^*) \pi_s r_{s,i} + \nu_i^* \pi_s r_{s,i} - \lambda_s^* + \eta_{s,i}^* & = 0 \\ \nu_i^* (\theta_i^* - \theta_{i,\min}) & = 0 \\ \lambda_s^* \left(1 - \sum_{i=1}^M x_{s,i}^* \right) & = 0 \\ \eta_{s,i}^* x_{s,i}^* & = 0 \end{aligned} \quad (3)$$

Rewriting the first of these equations, we get

$$\left(\frac{d}{d\theta_i} U_i(\theta_i^*) + \nu_i^* \right) r_{s,i} = \frac{1}{\pi_s} (\lambda_s^* - \eta_{s,i}^*)$$

From the fourth condition (a complementary slackness condition) among those in Equation (3), we see that whenever $\eta_{s,i}^* > 0$ it must hold that $x_{s,i}^* = 0$, hence, for the (s, i) such that $x_{s,i}^* > 0$ the following must be satisfied

$$\left(\frac{d}{d\theta_i} U_i(\theta_i^*) + \nu_i^* \right) r_{s,i} = \frac{1}{\pi_s} \lambda_s^*$$

i.e., that $\left(\frac{d}{d\theta_i} U_i(\theta_i^*) + \nu_i^* \right) r_{s,i}$ must be equalized across users i . It is this that motivates Equation (4) in our algorithm.

Note that, without the rate guarantee constraints, we get back the original fair scheduling algorithm. The above analysis

suggests that the way forward is to incorporate the rate guarantees via the corresponding Lagrange multipliers. Due to the additive manner in which the ν_i appear, we will call them *index biases*, as they *bias* the usual fair scheduling indices to encourage more frequent scheduling of the UEs that require rate guarantees.

B. Utility optimal scheduling with rate guarantees

Two small step-sizes $a > 0, b > 0$, with $b \ll a$ are chosen. In slot k , given the EWMA throughputs $\boldsymbol{\theta}^{(a,b)}(k)$, the index biases, $\nu_i^{(a,b)}(k) \geq 0, 1 \leq i \leq M$, and the joint channel state $s(k) \in \mathcal{S}$, determine $\mathbf{r}^*(\boldsymbol{\theta}^{(a,b)}(k), \boldsymbol{\nu}^{(a,b)}(k), s(k))$ as follows:

$$\begin{aligned} \mathbf{r}^*(\boldsymbol{\theta}^{(a,b)}(k), \boldsymbol{\nu}^{(a,b)}(k), s(k)) = & \arg \max_{\mathbf{r} \in \mathcal{R}_{s(k)}} (\nabla U(\boldsymbol{\theta}^{(a,b)}(k)) + \boldsymbol{\nu}^{(a,b)}(k))^T \cdot \mathbf{r} \end{aligned} \quad (4)$$

Update the EWMA throughputs as follows:

$$\begin{aligned} \boldsymbol{\theta}^{(a,b)}(k+1) & = \boldsymbol{\theta}^{(a,b)}(k) \\ & + a(\mathbf{r}^*(\boldsymbol{\theta}^{(a,b)}(k), \boldsymbol{\nu}^{(a,b)}(k), s(k)) - \boldsymbol{\theta}^{(a,b)}(k)) \end{aligned} \quad (5)$$

For all i , update the index biases as follows:

$$\nu_i^{(a,b)}(k+1) = \left[\nu_i^{(a,b)}(k) + b(\theta_{\min}^{(a,b)} - \theta_i^{(a,b)}(k)) \right]_0^{\nu_{\max}} \quad (6)$$

ν_{\max} is a suitably chosen value that is large enough so that the equilibrium values of the index-biases lie within $[0, \nu_{\max}]^M$. We will discuss a condition for ensuring this in Section IV-C

The above algorithm needs to be compared with a similar one provided in [9]. The difference lies in the recursion for the index bias, Equation (6). The recursion above is of the stochastic approximation type, whereas the one in [9] is similar to the recursion for a queue (called a *token counter* in that paper). Another difference is that in Equation (6) we use the EWMA throughput in the index-bias update, whereas in [9] just the rate allocated in the current slot is used; see Section V-A. In [9], the token counter is used in Equation (4) after multiplication by the same step-size, a , as is used in the EWMA throughput calculation.

IV. CONVERGENCE ANALYSIS

In Section IV-A, to provide insight, we give a rough sketch of the proof for two UEs. The rigorous proof of the formal convergence statement is provided in Section IV-B.

A. Outline of the convergence analysis: a two UE example

There are 2 UEs with $\theta_{0,\min} = 0$ and $\theta_{1,\min} > 0$. Hence, we only need to update the index bias $\nu_1(k), k \geq 0$. We have to analyze the following recursions:

$$\begin{aligned} \mathbf{r}(k) & = \arg \max_{\mathbf{r} \in \mathcal{R}_{s(k)}} \left[\frac{d}{d\theta_0} U(\theta_0(k)) \left(\frac{d}{d\theta_1} U(\theta_1(k)) + \nu_1(k) \right) \right] \cdot \mathbf{r} \end{aligned} \quad (7)$$

$$\boldsymbol{\theta}(k+1) = \boldsymbol{\theta}(k) + a(\mathbf{r}(k) - \boldsymbol{\theta}(k)) \quad (8)$$

$$\nu_1(k+1) = (\nu_1(k) + b(\theta_{1,\min} - \theta_1(k)))^+ \quad (9)$$

Notice that if $\theta_1(k+1) < \theta_{1,\min}$, the index bias $\nu_1(k+1)$ increases, thereby providing a larger bias in favour of UE_1 . This encourages the UE_1 throughput to go towards $\theta_{1,\min}$.

Since $b \ll a$, the index bias evolves slowly as compared to the EWMA throughput updates. Motivated by [6, Chapter 6] and [8, Section 8.6], we consider the index bias to be fixed at ν_1 , and define

$$\mathbf{r}^*(\boldsymbol{\theta}, \nu_1, s) = \arg \max_{\mathbf{r} \in \mathcal{R}_s} \left[\frac{d}{d\theta_0} U(\theta_0) \left(\frac{d}{d\theta_1} U(\theta_1) + \nu_1 \right) \right] \cdot \mathbf{r}$$

Since a is also small, in large time, the following o.d.e. can be considered to hold:

$$\dot{\boldsymbol{\theta}}(t) = \sum_{s \in \mathcal{S}} \pi_s \mathbf{r}^*(\boldsymbol{\theta}(t), \nu_1, s) - \boldsymbol{\theta}(t) \quad (10)$$

Denote the stationary point of this o.d.e. by $(\theta_{0,\infty}(\nu_1), \theta_{1,\infty}(\nu_1))$. Since $b \ll a$, the EWMA updates can be taken to have stabilized with respect to the slower index-bias updates. With this in mind, the index bias recursion in Equation (7) yields the following o.d.e. for the index bias for UE₁ (if we assume that $\nu_1(t) > 0$ for all t):

$$\dot{\nu}_1(t) = \theta_{1,\min} - \theta_{1,\infty}(\nu_1(t)) \quad (11)$$

The stationary point for this o.d.e. will yield

$$\theta_{1,\infty}(\nu_{1,\infty}) = \theta_{1,\min} \quad (12)$$

i.e., the limiting UE₁ throughput at the limiting index bias is $\theta_{1,\min}$.

We can infer that the following holds for the stationary point of the o.d.e. in Equation (10) with $\nu_1 = \nu_{1,\infty}$:

$$\begin{aligned} [\theta_{0,\infty}(\nu_{1,\infty}), \theta_{1,\infty}(\nu_{1,\infty})] &= \sum_{s \in \mathcal{S}} \pi_s \arg \max_{\mathbf{r} \in \mathcal{R}_s} \\ &\left[\frac{d}{d\theta_0} U(\theta_{0,\infty}(\nu_{1,\infty})) \left(\frac{d}{d\theta_1} U(\theta_{1,\infty}(\nu_{1,\infty})) + \nu_{1,\infty} \right) \right] \cdot \mathbf{r} \end{aligned} \quad (13)$$

It is easily seen that (see [2], [11]) under strict convexity of $\bar{\mathcal{R}}$ (see Condition 2), for any $\mathbf{x} \in \mathbf{R}_+^M$,

$$\arg \max_{\mathbf{r} \in \bar{\mathcal{R}}} \mathbf{x}^T \cdot \mathbf{r} = \sum_{s \in \mathcal{S}} \pi_s \arg \max_{\mathbf{r} \in \mathcal{R}_s} \mathbf{x}^T \cdot \mathbf{r} \quad (14)$$

Using Equation (14), we conclude that

$$\begin{aligned} [\theta_{0,\infty}(\nu_{1,\infty}), \theta_{1,\infty}(\nu_{1,\infty})] &= \arg \max_{\mathbf{r} \in \bar{\mathcal{R}}} \\ &\left[\frac{d}{d\theta_0} U(\theta_{0,\infty}(\nu_{1,\infty})) \left(\frac{d}{d\theta_1} U(\theta_{1,\infty}(\nu_{1,\infty})) + \nu_{1,\infty} \right) \right] \cdot \mathbf{r} \end{aligned} \quad (15)$$

For notational convenience, let us write $[\delta_0 \ \delta_1] := \left[\frac{d}{d\theta_0} U(\theta_{0,\infty}(\nu_{1,\infty})) \ \left(\frac{d}{d\theta_1} U(\theta_{1,\infty}(\nu_{1,\infty})) \right) \right]$. Then, Equation (15), implies that, for all $\mathbf{r} \in \bar{\mathcal{R}}$

$$\begin{aligned} [\delta_0 \ \delta_1 + \nu_{1,\infty}] \cdot [\theta_{0,\infty}(\nu_{1,\infty}) \ \theta_{1,\infty}(\nu_{1,\infty})]^T &\geq \\ [\delta_0 \ \delta_1 + \nu_{1,\infty}] \cdot \mathbf{r} & \\ [\delta_0 \ \delta_1] \cdot [\theta_{0,\infty}(\nu_{1,\infty}) \ \theta_{1,\infty}(\nu_{1,\infty})]^T & \\ + \nu_{1,\infty} \theta_{1,\infty}(\nu_{1,\infty}) &\geq [\delta_0 \ \delta_1] \cdot \mathbf{r} + \nu_{1,\infty} r_1 \\ \nu_{1,\infty} (\theta_{1,\min} - r_1) &\geq \\ [\delta_0 \ \delta_1] \cdot \left(\mathbf{r} - [\theta_{0,\infty}(\nu_{1,\infty}) \ \theta_{1,\infty}(\nu_{1,\infty})]^T \right) & \end{aligned} \quad (16)$$

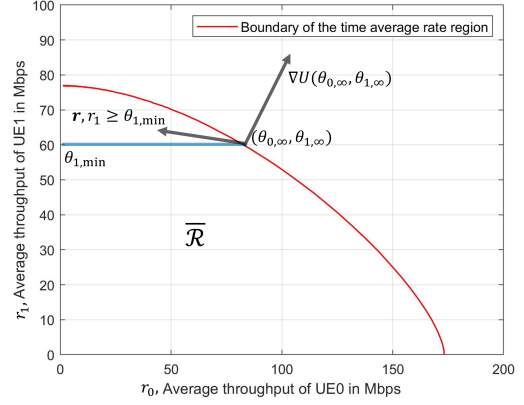


Fig. 1. Demonstration of the optimality of the o.d.e. limit. Two UEs at distances of 100 m and 200 m, system bandwidth 40 MHz, slot time 1 ms, gNB transmit power 100 mW.

where we have used Equation (12) in the left term of the inequality in the last line of the above sequence of inequalities.

It follows that, for $\mathbf{r} \in \bar{\mathcal{R}}$ with $r_1 \geq \theta_{1,\min}$, since $\nu_{1,\infty} \geq 0$, we have shown that (see Figure 1 for an illustration)

$$\begin{aligned} &\left[\frac{d}{d\theta_0} U(\theta_{0,\infty}(\nu_{1,\infty})) \left(\frac{d}{d\theta_1} U(\theta_{1,\infty}(\nu_{1,\infty})) \right) \right] \cdot \\ &\left(\mathbf{r} - [\theta_{0,\infty}(\nu_{1,\infty}), \theta_{1,\infty}(\nu_{1,\infty})]^T \right) \leq 0 \end{aligned} \quad (17)$$

Since $\bar{\mathcal{R}} \cap \{\mathbf{r} \in \mathbb{R}_+ : r_1 \geq \theta_{1,\min}\}$ is a closed convex set, and $U(\mathbf{r})$ is strictly concave, it follows from [5, Chapter 3, Page 103] that $[\theta_{0,\infty}(\nu_{1,\infty}), \theta_{1,\min}]$ is the unique utility maximising throughput vector with a rate guarantee for UE₁.

The above argument suggests that the sequence of EWMA throughputs will, in large time, become close to $[\theta_{0,\infty}(\nu_{1,\infty}), \theta_{1,\min}]$. This is formalized in the next section.

B. Main result on convergence with rate guarantees

In this section, under certain conditions, we analyze the algorithm defined by Equations (4)-(6) using the approach for weak convergence of two-time-scale constant step-size stochastic approximation provided in [8, Section 8.6]. We culminate this section in Theorem 1 which is the main convergence result for the Lagrange multipliers.

Define the sequence of σ -fields, $\mathcal{F}_0^{(a,b)}, \mathcal{F}_1^{(a,b)}, \dots, \mathcal{F}_k^{(a,b)}, \dots$, as follows:

$$\begin{aligned} \mathcal{F}_0^{(a,b)} &= \sigma(\boldsymbol{\theta}^{(a,b)}(0), \boldsymbol{\nu}^{(a,b)}(0)), \dots, \\ \mathcal{F}_k^{(a,b)} &= \sigma(\boldsymbol{\theta}^{(a,b)}(0), \boldsymbol{\nu}^{(a,b)}(0), s(0), \dots, \boldsymbol{\theta}^{(a,b)}(k), \boldsymbol{\nu}^{(a,b)}(k)) \end{aligned}$$

Further, define:

$$\begin{aligned} \mathbf{h}(\boldsymbol{\theta}^{(a,b)}(k), \boldsymbol{\nu}^{(a,b)}(k), s(k-1)) &:= \\ \mathbb{E} \left(\mathbf{r}^*(\boldsymbol{\theta}^{(a,b)}(k), \boldsymbol{\nu}^{(a,b)}(k), S(k)) | \mathcal{F}_k^{(a,b)} \right) \end{aligned} \quad (18)$$

and observe that \mathbf{h} does not depend on k or on (a, b) . The so-called martingale difference “noise” in the rate recursion (5) is defined by:

$$\begin{aligned} \mathbf{M}^{(a,b)}(k) &:= \mathbf{r}^*(\boldsymbol{\theta}^{(a,b)}(k), \boldsymbol{\nu}^{(a,b)}(k), s(k)) \\ &\quad - \mathbf{h}(\boldsymbol{\theta}^{(a,b)}(k), \boldsymbol{\nu}^{(a,b)}(k), s(k-1)). \end{aligned} \quad (19)$$

For the index-bias recursion (6), we define

$$\mathbf{g}(\boldsymbol{\theta}) := \boldsymbol{\theta}_{\min} - \boldsymbol{\theta} \quad (20)$$

with the associated martingale difference noise being zero. With these definitions, we rewrite Equations (5)-(6) as follows:

$$\begin{aligned} \boldsymbol{\theta}^{(a,b)}(k+1) &= \boldsymbol{\theta}^{(a,b)}(k) \\ &\quad + a \left(\mathbf{h}(\boldsymbol{\theta}^{(a,b)}(k), \boldsymbol{\nu}^{(a,b)}(k), s(k-1)) \right. \\ &\quad \left. - \boldsymbol{\theta}^{(a,b)}(k) + \mathbf{M}^{(a,b)}(k) \right) \end{aligned} \quad (21)$$

$$\boldsymbol{\nu}^{(a,b)}(k+1) = \left[\boldsymbol{\nu}^{(a,b)}(k) + b \mathbf{g}(\boldsymbol{\theta}^{(a,b)}(k)) \right]_0^{\nu_{\max}} \quad (22)$$

The result we will apply is [8, Theorem 8.6.1]. To apply this result, we proceed to verify that the conditions A8.6.0 to A8.6.5 (in [8, Section 8.6.1]) hold in our problem.

A8.6.0 The projection applied to the index-bias $\boldsymbol{\nu}^{(a,b)}(k)$ is on a hyperrectangle, of the type described in [8, A 4.3.1].

A8.6.1 We notice that $\mathcal{R}_s \subset \mathbb{R}_+^M$ are compact sets, and $\mathbf{r}^*(\boldsymbol{\theta}, \boldsymbol{\nu}, s(k)) \in \mathcal{R}_{s(k)} \subset \bar{\mathcal{R}}$ for each k . Further, by rewriting Equation (5) as follows,

$$\begin{aligned} \boldsymbol{\theta}^{(a,b)}(k+1) &= \\ (1-a)\boldsymbol{\theta}^{(a,b)}(k) &+ a \mathbf{r}^*(\boldsymbol{\theta}^{(a,b)}(k), \boldsymbol{\nu}^{(a,b)}(k), s(k)), \end{aligned} \quad (23)$$

we observe that $\boldsymbol{\theta}^{(a,b)}(k+1)$ will always be in a compact set, and uniform integrability of the family of random vectors $\{\mathbf{r}^*(\boldsymbol{\theta}^{(a,b)}(k), \boldsymbol{\nu}^{(a,b)}(k), s(k)) - \boldsymbol{\theta}^{(a,b)}(k)\}, (a, b), k\}$, where the random vectors are indexed by (a, b) and k , holds. It follows that

$$\left\{ \mathbf{h}(\boldsymbol{\theta}^{(a,b)}(k), \boldsymbol{\nu}^{(a,b)}(k), s(k-1)) - \boldsymbol{\theta}^{(a,b)}(k), \mathbf{g}(\boldsymbol{\theta}^{(a,b)}(k)), \right. \\ \left. (a, b), k \right\}$$

is uniformly integrable, and moreover, for each fixed $\boldsymbol{\theta}$ and $\boldsymbol{\nu}$,

$$\left\{ \mathbf{h}(\boldsymbol{\theta}, \boldsymbol{\nu}, s(k-1)) - \boldsymbol{\theta}, \mathbf{g}(\boldsymbol{\theta}), (a, b), k \right\}$$

is also uniformly integrable.

We further require that the sequence of random variables $S(k), k \geq 0$ is tight. Condition 1 below implies this.

Condition 1: Assume that the channel state process $S(k), k \geq 0$, belongs to a compact set in \mathbb{R}^M . \square

A8.6.2 We need the continuity of $(\mathbf{h}(\boldsymbol{\theta}, \boldsymbol{\nu}, s) - \boldsymbol{\theta})$ uniformly over (a, b) and s . Here, the (a, b) do not matter; we need the continuity of $(\mathbf{h}(\boldsymbol{\theta}, \boldsymbol{\nu}, s) - \boldsymbol{\theta})$ over $\boldsymbol{\theta}, \boldsymbol{\nu}$ uniformly in s .

Following [2], we require:

Condition 2 (Strict Convexity of Rate Regions): Assume that for every $\mathbf{a} \in \mathbb{R}_+^M$, and $s \in \mathcal{S}$, $\arg \max_{\mathbf{r} \in \mathcal{R}_{|s}} \mathbf{a} \cdot \mathbf{r}$ is unique, and, also, $\arg \max_{\mathbf{r} \in \bar{\mathcal{R}}} \mathbf{a} \cdot \mathbf{r}$ is unique. \square

The strict convexity is understood to apply to the Pareto optimal boundary of the rate regions.

Further, we require:

Condition 3: Assume that for $(\mathbf{a}, s) \in \mathbb{R}_+^M \times \mathcal{S}$, the mappings $(\mathbf{a}, s) \mapsto \arg \max_{\mathbf{r} \in \bar{\mathcal{R}}_{|s}} \mathbf{a} \cdot \mathbf{r}$ and $\mathbf{a} \mapsto \arg \max_{\mathbf{r} \in \bar{\mathcal{R}}} \mathbf{a} \cdot \mathbf{r}$ are continuous. \square

If the \mathcal{R}_s is polyhedral for each $s \in \mathcal{S}$, Condition 3 may hold if \mathcal{S} is a continuum², for example when we are dealing with Rayleigh fading with truncation to a compact set (in view of Condition 1).

Analogous to (14), using Condition 2, it is easily seen that (see [2]):

$$\arg \max_{\mathbf{r} \in \bar{\mathcal{R}}_{|s}} \mathbf{a}^T \cdot \mathbf{r} = \sum_{s \in \mathcal{S}} P(s'|s) \arg \max_{\mathbf{r} \in \mathcal{R}_{s'}} \mathbf{a}^T \cdot \mathbf{r} \quad (24)$$

Since $(\nabla U(\boldsymbol{\theta}) + \boldsymbol{\nu})^T$ is continuous in $(\boldsymbol{\theta}, \boldsymbol{\nu})$, Condition 3 and the compactness of \mathcal{S} implies that $\mathbf{h}(\boldsymbol{\theta}, \boldsymbol{\nu}, s) - \boldsymbol{\theta}$ is continuous over $(\boldsymbol{\theta}, \boldsymbol{\nu})$ uniformly in s .

Trivially, $\mathbf{g}(\boldsymbol{\theta})$ is continuous in $\boldsymbol{\theta}$.

A8.6.3 Fix $(\boldsymbol{\theta}, \boldsymbol{\nu})$. Consider the following (notice that the step sizes (a, b) do not play any role) for a suitable continuous function $\bar{\mathbf{h}}(\boldsymbol{\theta}, \boldsymbol{\nu})$:

$$\begin{aligned} &\lim_{\substack{n, m \rightarrow \infty \\ a \rightarrow 0 \\ b \rightarrow 0}} \frac{1}{m} \sum_{i=n}^{n+m-1} \left(\mathbb{E} \left(\mathbf{h}(\boldsymbol{\theta}, \boldsymbol{\nu}, S(i-1)) - \boldsymbol{\theta} | \mathcal{F}_n^{(a,b)} \right) - \bar{\mathbf{h}}(\boldsymbol{\theta}, \boldsymbol{\nu}) \right) \\ &= \lim_{(n, m \rightarrow \infty)} \frac{1}{m} \sum_{i=n}^{n+m-1} \left(\mathbb{E} \left(\mathbf{r}^*(\boldsymbol{\theta}, \boldsymbol{\nu}, S(i)) - \boldsymbol{\theta} | \mathcal{F}_n^{(a,b)} \right) - \bar{\mathbf{h}}(\boldsymbol{\theta}, \boldsymbol{\nu}) \right) \\ &= \lim_{(m \rightarrow \infty)} \frac{1}{m} \sum_{i=1}^m \left(\mathbb{E} \left(\mathbf{r}^*(\boldsymbol{\theta}, \boldsymbol{\nu}, S(i)) - \boldsymbol{\theta} | s(0) \right) - \bar{\mathbf{h}}(\boldsymbol{\theta}, \boldsymbol{\nu}) \right) \\ &= \mathbb{E}_{\infty} \mathbf{r}^*(\boldsymbol{\theta}, \boldsymbol{\nu}, S) - \boldsymbol{\theta} - \bar{\mathbf{h}}(\boldsymbol{\theta}, \boldsymbol{\nu}) \end{aligned}$$

in probability, where we have used ergodicity of the Markov chain of channel states and the uniform integrability of $\{\mathbf{r}^*(\boldsymbol{\theta}, \boldsymbol{\nu}, S(i)) | s(0), i \geq 1\}$ in the last equality and $\mathbb{E}_{\infty}(\cdot)$ refers to the expectation with respect to the stationary distribution of the Markov chain. It follows that, for the last term in the above sequence of equalities to be equal to 0,

$$\begin{aligned} \bar{\mathbf{h}}(\boldsymbol{\theta}, \boldsymbol{\nu}) &= \mathbb{E}_{\infty} \mathbf{r}^*(\boldsymbol{\theta}, \boldsymbol{\nu}, S) - \boldsymbol{\theta} \\ &= \arg \max_{\mathbf{r} \in \bar{\mathcal{R}}} (\nabla U(\boldsymbol{\theta}) + \boldsymbol{\nu}^T) \cdot \mathbf{r} - \boldsymbol{\theta} \end{aligned} \quad (25)$$

is the desired function. The second equality requires Condition 2, and the continuity of $\bar{\mathbf{h}}(\boldsymbol{\theta}, \boldsymbol{\nu})$ with respect to $(\boldsymbol{\theta}, \boldsymbol{\nu})$ follows from Condition 3.

A8.6.4 We now need to show that, for fixed $\boldsymbol{\nu}$, the o.d.e.

$$\dot{\boldsymbol{\theta}}(t) = \bar{\mathbf{h}}(\boldsymbol{\theta}(t), \boldsymbol{\nu}) \quad (26)$$

has a unique globally asymptotically stable point that is continuous in $\boldsymbol{\nu}$, characterized by

$$\boldsymbol{\theta}_{\infty}(\boldsymbol{\nu}) = \arg \max_{\mathbf{r} \in \bar{\mathcal{R}}} (\nabla U(\boldsymbol{\theta}_{\infty}(\boldsymbol{\nu})) + \boldsymbol{\nu}^T) \cdot \mathbf{r} \quad (27)$$

We first argue that the rest point of the dynamics (26) is unique for each $\boldsymbol{\nu} \in \mathbb{R}_+^M$, and that the rest point is $\boldsymbol{\theta}_{\infty}(\boldsymbol{\nu})$.

²In the sequel, we will continue to use the notation $\sum_{s \in \mathcal{S}} (\cdot)$ and $P(\cdot | s)$ with the understanding that these should be interpreted as integrals and transition kernel densities, respectively, when \mathcal{S} is a continuum.

Consider the optimization problem $\max_{\mathbf{r} \in \overline{\mathcal{R}}} (U(\mathbf{r}) + \boldsymbol{\nu}^T \cdot \mathbf{r})$. This is the maximization of a strictly concave function over a convex set; hence, the solution, say $\mathbf{r}^*(\boldsymbol{\nu})$, is unique. Further, this optimum solution must satisfy $(\nabla U(\mathbf{r}^*(\boldsymbol{\nu})) + \boldsymbol{\nu})^T \cdot (\mathbf{r} - \mathbf{r}^*(\boldsymbol{\nu})) \leq 0$ for all $\mathbf{r} \in \overline{\mathcal{R}}$; i.e., $\mathbf{r}^*(\boldsymbol{\nu}) = \arg \max_{\mathbf{r} \in \overline{\mathcal{R}}} (\nabla U(\mathbf{r}^*(\boldsymbol{\nu})) + \boldsymbol{\nu})^T \cdot \mathbf{r}$. Observe from (27) that this $\mathbf{r}^*(\boldsymbol{\nu}) = \boldsymbol{\theta}_\infty(\boldsymbol{\nu})$, so the right-hand-side of (25) is zero at $\boldsymbol{\theta} = \boldsymbol{\theta}_\infty(\boldsymbol{\nu})$, and hence $\boldsymbol{\theta}_\infty(\boldsymbol{\nu})$ is the unique rest point for the o.d.e. (26).

In the Appendix, we show that $\boldsymbol{\theta}_\infty(\boldsymbol{\nu})$ is globally asymptotically stable for the o.d.e. (26).

Continuity of the unique stable point $\boldsymbol{\theta}_\infty(\boldsymbol{\nu})$ with $\boldsymbol{\nu}$: Continuing the previous argument, we have $\mathbf{r}^*(\boldsymbol{\nu}) = \arg \max_{\mathbf{r} \in \overline{\mathcal{R}}} (\nabla U(\mathbf{r}^*(\boldsymbol{\nu})) + \boldsymbol{\nu})^T \cdot \mathbf{r}$. Consider the sequence, indexed by $k \geq 1$, $\boldsymbol{\nu}_k \rightarrow_{k \rightarrow \infty} \boldsymbol{\nu}_0$ in \mathbb{R}_+^M . For every $k \geq 1$, $\mathbf{r}^*(\boldsymbol{\nu}_k) \in \overline{\mathcal{R}}$, a compact set. Thus, consider a subsequence $\mathbf{r}^*(\boldsymbol{\nu}_{k_j}) \rightarrow_{j \rightarrow \infty} \mathbf{r}'$ and $\boldsymbol{\nu}_{k_j} \rightarrow_{j \rightarrow \infty} \boldsymbol{\nu}_0$. Since $U(\boldsymbol{\theta})$ is continuously differentiable, $\nabla U(\mathbf{r}^*(\boldsymbol{\nu}_{k_j})) + \boldsymbol{\nu}_{k_j} \rightarrow_{j \rightarrow \infty} \nabla U(\mathbf{r}') + \boldsymbol{\nu}_0$. Hence, by Condition 2,

$$\begin{aligned} & \lim_j \arg \max_{\mathbf{r} \in \overline{\mathcal{R}}} (\nabla U(\mathbf{r}^*(\boldsymbol{\nu}_{k_j})) + \boldsymbol{\nu}_{k_j})^T \cdot \mathbf{r} \\ &= \arg \max_{\mathbf{r} \in \overline{\mathcal{R}}} (\nabla U(\mathbf{r}') + \boldsymbol{\nu}_0)^T \cdot \mathbf{r}; \end{aligned}$$

i.e., $\mathbf{r}^*(\boldsymbol{\nu}_{k_j}) \rightarrow_{j \rightarrow \infty} \arg \max_{\mathbf{r} \in \overline{\mathcal{R}}} (\nabla U(\mathbf{r}') + \boldsymbol{\nu}_0)^T \cdot \mathbf{r}$, or $\mathbf{r}' = \arg \max_{\mathbf{r} \in \overline{\mathcal{R}}} (\nabla U(\mathbf{r}') + \boldsymbol{\nu}_0)^T \cdot \mathbf{r}$. By the uniqueness, proved above, $\mathbf{r}' = \mathbf{r}^*(\boldsymbol{\nu}_0)$. This holds for every convergent subsequence of $\{\mathbf{r}^*(\boldsymbol{\nu}_k), k \geq 1\}$. Hence, $\mathbf{r}^*(\boldsymbol{\nu}_k) \rightarrow_{k \rightarrow \infty} \mathbf{r}^*(\boldsymbol{\nu}_0)$, and we conclude that $\boldsymbol{\theta}_\infty(\boldsymbol{\nu})$ is continuous in $\boldsymbol{\nu}$.

A8.6.5 We first need to show uniform integrability of the sequence $\{\mathbf{g}(\boldsymbol{\theta}_\infty(\boldsymbol{\nu}^{(a,b)}(k))), (a,b), k\}$, and, for each $\boldsymbol{\nu}$, of the sequence $\{\mathbf{g}(\boldsymbol{\theta}_\infty(\boldsymbol{\nu})), (a,b)\}$. The first follows because the sequence belong to a compact set. The second is trivial because \mathbf{g} is independent of (a,b) .

Further, we must show that there is a continuous function $\boldsymbol{\nu} \mapsto \overline{\mathbf{g}}(\boldsymbol{\theta}_\infty(\boldsymbol{\nu}), \boldsymbol{\nu})$ such that for each $\boldsymbol{\nu}$, in probability, the following holds:

$$\begin{aligned} & \lim_{\substack{n,m \rightarrow \infty \\ a \rightarrow 0 \\ \frac{b}{a} \rightarrow 0}} \frac{1}{m} \sum_{i=n}^{n+m-1} \left(\mathbb{E} \left(\mathbf{g}(\boldsymbol{\theta}_\infty(\boldsymbol{\nu}), \boldsymbol{\nu}) | \mathcal{F}_n^{(a,b)} \right) - \overline{\mathbf{g}}(\boldsymbol{\theta}_\infty(\boldsymbol{\nu}), \boldsymbol{\nu}) \right) \\ &= 0 \end{aligned}$$

i.e.,

$$\lim_{\substack{n,m \rightarrow \infty \\ a \rightarrow 0 \\ \frac{b}{a} \rightarrow 0}} \frac{1}{m} \sum_{i=n}^{n+m-1} (\boldsymbol{\theta}_{\min} - \boldsymbol{\theta}_\infty(\boldsymbol{\nu})) - \overline{\mathbf{g}}(\boldsymbol{\theta}_\infty(\boldsymbol{\nu}), \boldsymbol{\nu}) = 0$$

It follows that the desired function is

$$\overline{\mathbf{g}}(\boldsymbol{\theta}_\infty(\boldsymbol{\nu}), \boldsymbol{\nu}) = \boldsymbol{\theta}_{\min} - \boldsymbol{\theta}_\infty(\boldsymbol{\nu}) \quad (28)$$

which is continuous in $\boldsymbol{\nu}$ by A8.6.4.

The following condition on the optimization problem in Equation (1) ensures that we can restrict $\boldsymbol{\nu}$ to a compact set:

Condition 4: There is a $\nu_{\max} > 0$ such that the optimum Lagrange multipliers (dual variables) of the optimization problem (1) lie in the set $[0, \nu_{\max}]^M$. \square

In the Appendix, we illustrate how this condition can be checked, by providing an example of a two UE problem.

With all the above conditions having been met, along with the o.d.e. in Equation (26), [8, Theorem 8.6.1] considers the following o.d.e. for the index-bias

$$\dot{\boldsymbol{\nu}}(t) = \boldsymbol{\theta}_{\min} - \boldsymbol{\theta}_\infty(\boldsymbol{\nu}(t)) + \boldsymbol{\xi}(t), \quad t \geq 0 \quad (29)$$

where $\boldsymbol{\xi}(t) \in -C(\boldsymbol{\nu}(t))$ is the term that compensates for the dynamics so that $\boldsymbol{\nu}(t)$ stays in its constraint set; here $C(\boldsymbol{\nu})$ is the cone of outward normals to the constraint set at $\boldsymbol{\nu}$.

Let L denote the set of limit points of the dynamics (29) in $[0, \nu_{\max}]^M$ over all initial conditions. For a $\delta > 0$, let $L^{(\delta)}$ denote the δ -neighborhood of L . Define the continuous time interpolation $\hat{\boldsymbol{\nu}}^{(a,b)}(t)$ for $t \geq 0$ as:

$$\hat{\boldsymbol{\nu}}^{(a,b)}(t) = \boldsymbol{\nu}^{(a,b)}(k), \quad t \in [bk, b(k+1)).$$

The foregoing has established the following theorem.

Theorem 1: Let q_a be any sequence of integers such that $aq_a \rightarrow \infty$ as $a \rightarrow 0$. For the model considered in this paper, under Conditions 1, 2, 3, and 4, there exist $T_a \rightarrow \infty$ as $a \rightarrow 0$ such that for every $\delta > 0$, we have

$$\lim_{\substack{b/a \rightarrow 0 \\ a \rightarrow 0}} P \left\{ \hat{\boldsymbol{\nu}}^{(a,b)}(aq_a + t) \notin L^{(\delta)}, \text{ for some } t \leq T_a \right\} = 0. \quad (30)$$

Proof: All assumptions A8.6.0 to A8.6.5, in order to apply [8, Theorem 8.6.1], have been verified above, and the theorem follows. \blacksquare

C. Stable rest points and the optimum solution

We now use properties of the joint stable points of the o.d.e. in Equation (26) and the o.d.e. in Equation (29), i.e., $(\boldsymbol{\theta}_\infty(\boldsymbol{\nu}_\infty), \boldsymbol{\nu}_\infty)$, to show that these correspond to the optimal solution of the optimization problem in Equation (1).

Consider a stable rest point $\boldsymbol{\nu}_\infty$ of the o.d.e. in Equation (29). Such a rest point is in L . Using Equation (27), we can write, for every $\mathbf{r} \in \overline{\mathcal{R}}$:

$$(\nabla U(\boldsymbol{\theta}_\infty(\boldsymbol{\nu}_\infty)) + \boldsymbol{\nu}_\infty)^T \cdot (\boldsymbol{\theta}_\infty(\boldsymbol{\nu}_\infty) - \mathbf{r}) \geq 0$$

Transposing, we obtain, for every $\mathbf{r} \in \overline{\mathcal{R}}$:

$$\begin{aligned} & \boldsymbol{\nu}_\infty^T \cdot (\boldsymbol{\theta}_\infty(\boldsymbol{\nu}_\infty) - \mathbf{r}) \geq \\ & (\nabla U(\boldsymbol{\theta}_\infty(\boldsymbol{\nu}_\infty)))^T \cdot (\mathbf{r} - \boldsymbol{\theta}_\infty(\boldsymbol{\nu}_\infty)) \end{aligned} \quad (31)$$

Since $\boldsymbol{\nu}_\infty$ is stable rest point for the o.d.e. in Equation (29), and $\boldsymbol{\xi}(t) \in -C(\boldsymbol{\nu}(t))$, it follows that, for $1 \leq i \leq M$ (the number of UEs):

$$\begin{aligned} (\boldsymbol{\nu}_\infty)_i > 0 & \Rightarrow (\boldsymbol{\xi}_\infty)_i = 0 \quad \text{and} \quad \theta_{i,\min} = (\boldsymbol{\theta}_\infty(\boldsymbol{\nu}_\infty))_i \\ (\boldsymbol{\nu}_\infty)_i = 0 & \Rightarrow (\boldsymbol{\xi}_\infty)_i \neq 0 \quad \text{and} \quad \theta_{i,\min} < (\boldsymbol{\theta}_\infty(\boldsymbol{\nu}_\infty))_i \end{aligned} \quad (32)$$

Note that the case $(\boldsymbol{\nu}_\infty)_i = 0, \theta_{i,\min} > (\boldsymbol{\theta}_\infty(\boldsymbol{\nu}_\infty))_i$ cannot be a stable rest point of the o.d.e. Equation (29).

Returning to Equation (31), and utilising Equations (32), we conclude that for $\mathbf{r} \in \overline{\mathcal{R}} \cap \{\mathbf{r} \in \mathbb{R}_+^M : \mathbf{r} \geq \boldsymbol{\theta}_{\min}\}$,

$$0 \geq (\nabla U(\boldsymbol{\theta}_\infty(\boldsymbol{\nu}_\infty)))^T \cdot (\mathbf{r} - \boldsymbol{\theta}_\infty(\boldsymbol{\nu}_\infty))$$

From [5, Chapter 3, Page 103], we see that $(\boldsymbol{\theta}_\infty(\boldsymbol{\nu}_\infty), \boldsymbol{\nu}_\infty)$ are optimal for the optimization problem in Equation (1). Since the optimization is one of a strictly concave function over a convex set, the solution is unique, and $\boldsymbol{\nu}_\infty$ is the correct set of Lagrange multipliers.

Thus $(\boldsymbol{\theta}_\infty(\boldsymbol{\nu}_\infty), \boldsymbol{\nu}_\infty)$ is a joint unique stable rest point for the joint o.d.e. system in Equation (26), with $\boldsymbol{\nu}$ replaced by $\boldsymbol{\nu}(t)$, and Equation (29).

We have already seen, in the verification of A8.6.4, that, for fixed index-bias $\boldsymbol{\nu}$, the EWMA rate recursion yields the o.d.e. in Equation (26) which has the unique globally asymptotically stable point $\boldsymbol{\theta}_\infty(\boldsymbol{\nu})$, characterized in Equation (27), and continuous in $\boldsymbol{\nu}$. Further, the index-bias recursion yields the o.d.e. in Equation (29). Theorem 1 establishes that if, in addition, $L = \{\boldsymbol{\nu}_\infty\}$, then, for large k , $(\boldsymbol{\theta}^{(a,b)}(k), \boldsymbol{\nu}^{(a,b)}(k))$ are close to $(\boldsymbol{\theta}_\infty(\boldsymbol{\nu}_\infty), \boldsymbol{\nu}_\infty)$, which solve the optimization problem in Equation (1). In other words, the throughput iterates converge to the optimum solution. A note of caution however is that L could contain limit cycles for the dynamics in (29). In the simulation experiments, we see that we do not have such issues on the examples considered.

V. SIMULATION EXPERIMENTS

We will carry out simulation experiments for the utility function $U_i(r_i) = \ln(1 + r_i)$, which satisfies all the mathematical properties in our earlier development. With a slight abuse of terminology, we will call the resulting rate allocation *proportionally fair*, even though the addition of a 1 to the rate r_i is a deviation from the commonly accepted $\ln r_i$. For modern wireless networks, the rates available to UEs are very high (several 10s of Mbps); the addition of the 1 will not result in a significant difference in the final rate allocation, and $\ln(1 + r_i)$ reduces mathematical complexities. The rate allocation algorithm with rate guarantees, presented in Section III-B will be referred to as PF-RG-LM (Proportional Fair scheduling with Rate Guarantees, using the Lagrange Multiplier approach).

A. The PF-RG-TC algorithm

In [3], [9], Mandelli et al. have also provided an index-bias based algorithm. They maintain a token counter (denoted, here, by $\tau(k)$) which is used to bias the rate allocation index. We call their algorithm PF-RG-TC (for Token Counter). Following the notation in Equations (4), (5), and (6), we write the PF-RG-TC as follows.

There is a single small step-size $a > 0$. At the beginning of slot k , given the joint channel state $s(k) \in \mathcal{S}$, the EWMA throughputs $\boldsymbol{\theta}^{(a)}(k)$, and the token counters $\tau_i^{(a)}(k) \geq 0, 1 \leq i \leq M$, determine $\mathbf{r}^*(\boldsymbol{\theta}^{(a)}(k), \boldsymbol{\tau}^{(a)}(k), s(k))$ as follows (see [9, Equations (4) and (5)]):

$$\mathbf{r}^*(\boldsymbol{\theta}^{(a)}(k), \boldsymbol{\tau}^{(a)}(k), s(k)) = \arg \max_{\mathbf{r} \in \mathcal{R}_s(k)} (\nabla U(\boldsymbol{\theta}^{(a)}(k)) + a\boldsymbol{\tau}^{(a)}(k))^T \cdot \mathbf{r} \quad (33)$$

The EWMA throughputs are updated as follows.

$$\begin{aligned} \boldsymbol{\theta}^{(a)}(k+1) &= \\ \boldsymbol{\theta}^{(a)}(k) + a(\mathbf{r}^*(\boldsymbol{\theta}^{(a)}(k), \boldsymbol{\tau}^{(a)}(k), s(k)) - \boldsymbol{\theta}^{(a)}(k)) \end{aligned} \quad (34)$$

For all i , the index biases are updated as follows.

$$\begin{aligned} \tau^{(a)}(k+1) &= \\ \left[\tau^{(a)}(k) + (\boldsymbol{\theta}_{\min}^{(a)} - \mathbf{r}^*(\boldsymbol{\theta}^{(a)}(k), \boldsymbol{\tau}^{(a)}(k), s(k))) \right]_0^{\tau_{\max}} \end{aligned} \quad (35)$$

In Section V-D, for two UEs we provide a performance comparison of PF-RG-LM and PF-RG-TC. In Section V-E we provide a simulation study of PF-RG-LM for more than two UEs.

B. Wireless communication model

All our simulations are for the following generic wireless communication setting. The channel is in the 2.4 GHz band, and the system bandwidth is $W = 40$ MHz. The noise floor is taken as Noise = -97 dBm; there are no interferers. For the BS transmit power P dBm, the mean received power at distance d m is given by $P - 42 - (30 \times \log_{10} d)$, where 42 is the attenuation at 1 m, and the pathloss exponent is 3. Rayleigh fading is assumed, which results in exponentially distributed attenuation in dB, with parameter 1. The slot duration is 0.001 sec.

In slot k , the received signal strengths $\text{RSS}_i(k), i \in \{0, 1\}$, are sampled as above. Then, the rates available to the two UEs are obtained independently (in time and across the UEs) from the Shannon channel capacity formula as follows:

$$r_{i,s(k)} = W \log_2 \left(1 + 10^{\left(\frac{\text{RSS}_i - \text{Noise}}{10} \right)} \right)$$

C. Two UEs: Rate regions

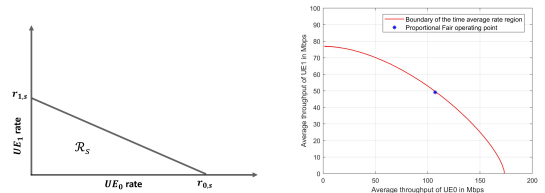


Fig. 2. Left plot: A slot rate region \mathcal{R}_s . Right plot: The rate region $\bar{\mathcal{R}}$.

There are two UEs, UE_0 and UE_1 , at the distances of 100 m and 200 m from the gNB. With the wireless channel model in Section V-B, and $P = 20$ dBm, the rate region in a slot, $\mathcal{R}_s, s \in \mathcal{S}$, has the triangular shape depicted in the left panel Figure 2. For such a rate region for two UEs, when the calculation in Equation (4) is done, it is of the form $\arg \max_{(r_0, r_1) \in \mathcal{R}_s} (a_0 r_0 + a_1 r_1)$ for some $(a_0, a_1) \geq \mathbf{0}$. Due to the shape of \mathcal{R}_s , this will result in one of the two UEs being scheduled in each slot.

The rate region, time averaged over all channel states, $\bar{\mathcal{R}}$, is shown in the right panel of Figure 2, along with the proportional fair operating point (for the utility $U_i(r_i) = \ln(1 + r_i)$). The outer boundary of $\bar{\mathcal{R}}$ has been obtained by simulating the

above wireless channel model for 10^6 slots, and obtaining the operating points for the utility $w_0r_0 + w_1r_1$ for a range of values of (w_0, w_1) .

D. Two UEs: Index-bias smoothing, & slow time scale updates

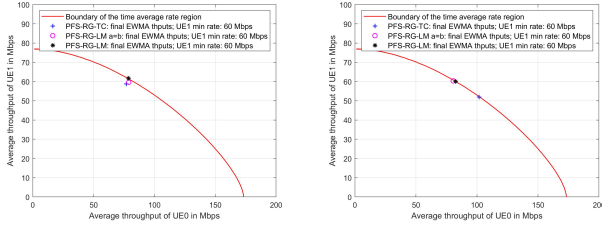


Fig. 3. PF-RG-TC, PF-RG-LM with $a = b$, and PF-RG-LM: Left plots $a = 0.0005, b = 0.000005$; Right plots $a = 0.00005, b = 0.0000005$. UE_1 rate guarantee 60 Mbps. The final rate pairs provided by the three algorithms superimposed on $\bar{\mathcal{R}}$.

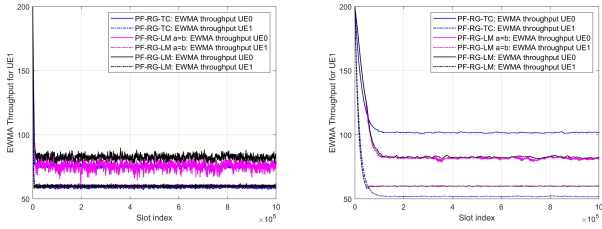


Fig. 4. PF-RG-TC, PF-RG-LM with $a = b$, and PF-RG-LM: Left plots $a = 0.0005, b = 0.000005$; Right plots $a = 0.00005, b = 0.0000005$. UE_1 rate guarantee 60 Mbps. Time series of EWMA throughputs (plots are in color).

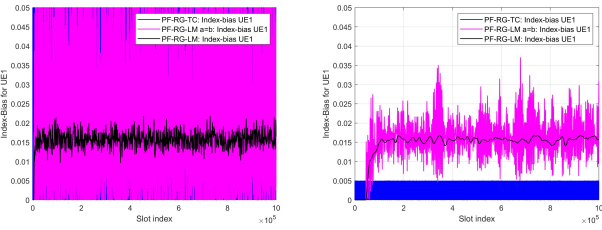


Fig. 5. PF-RG-TC, PF-RG-LM with $a = b$, and PF-RG-LM: Left plots $a = 0.0005, b = 0.000005$; Right plots $a = 0.00005, b = 0.0000005$. UE_1 rate guarantee 60 Mbps. Time series of index-biases (plots are in color).

In Figures 3, 4, and 5 we show the results from running the PF-RG-LM (with $b \ll a$, and $b = a$), and PF-RG-TC algorithms on rate data generated by the wireless communication model described in Section V-B, with the BS transmit power set at 100 mW. With $a = 0.0005, b = 0.000005$ (left plots) all three approaches provide an average rate of about 60 Mbps to UE_1 , but PF-RG-TC and PF-RG-LM (with $a = b$) provide lower rates to UE_0 . Figure 5 shows that the index-bias for PF-RG-TC fluctuates wildly, not appearing to follow any trend; with $a = b$, PF-RG-LM provides a slightly more controlled but still highly fluctuating index-bias. With the index-bias being

updated at a much slower time-scale than the EWMA rates, the index-bias for PF-RG-LM fluctuates slowly around a steady-state value. With $a = 0.00005, b = 0.0000005$ (right plots) the throughputs provided by PF-RG-TC are far from optimum. PF-RG-LM with $a = b$ and $b \ll a$ both provide accurate tracking of the optimum operating point. The index-bias for PF-RG-LM with $a = b$ is better controlled but still fluctuates significantly. On the other hand with a slower time-scale update, PF-RG-LM not only provides an accurate tracking of the optimum EWMA throughputs, but hovers around a value of approximately 0.016.

We may infer that the two-time scale stochastic approximation algorithm used in PF-RG-LM provides not only an accurate throughput operating point with rate guarantees, but also an accurate tracking of the Lagrange multipliers. We notice, from Equation (35), that in PF-RG-TC, in addition to stochastic approximation not being used in the token counter update, the token counter is updated by the rate allocation in the previous slot, rather than the EWMA rate, as in PF-RG-LM (see Equation (6)).

E. PF-RG-LM with $N(> 2)$ UEs

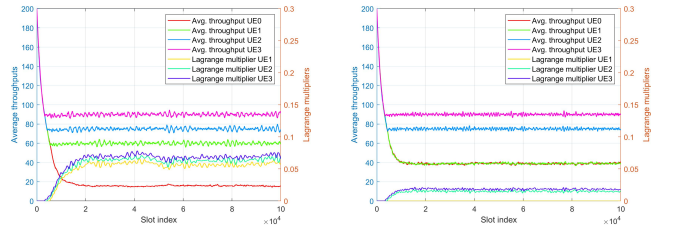


Fig. 6. PF-RG-LM with $a = 0.0005, b = 0.000005$, four UEs, at 200 m, with rate guarantees 0, 60, 75, 90 Mbps (left plot), and 0, 0, 75, 90 (right plot). The plots (in color) show the time series of the EWMA throughputs of the four UEs, and $\nu_i(k), 2 \leq i \leq 4$.

In Figure 6, we provide results from running PF-RG-LM on rate data generated from the wireless communication model described in Section V-B, with 4 UEs, all at 200 m from the BS, and the BS transmit power set at 1000 mW. In the left plot, the rate guarantees are 0, 60, 75, 90 Mbps for UE_0, UE_1, UE_2 , and UE_3 , and in the right plot these are 0, 0, 75, 90. Both plots show that the UEs with rate guarantees obtain their respective guaranteed rates. In the left plot, UE_0 achieves a rate of a little over 15 Mbps, whereas for the case in the right plot, UE_0 and UE_1 achieve the same rate of about 40 Mbps. The Lagrange multipliers also stabilize, with the larger guaranteed rate corresponding to the larger Lagrange multipliers, as expected. Notice that, in the right plot $\nu_1(k) = 0$ for all k .

F. Polyhedral average rate region, $\bar{\mathcal{R}}$

Figure 7 shows that the algorithms with and without rate guarantees work correctly even when the rate region, $\bar{\mathcal{R}}$, is not strictly convex. In the left plot, the channel has one state, i.e., $\mathcal{S} = \{s'\}$, $\bar{\mathcal{R}} = \mathcal{R}_{s'}$ and, in each slot one of the UEs

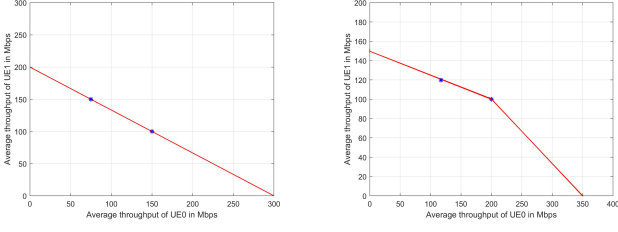


Fig. 7. Left plot: Two UEs, rate region with fixed rates 300 Mbps and 200 Mbps (i.e., the channel has only one state). Shown also are the PF throughputs, and the PF-RG-LM throughputs with RG of 150 Mbps for UE₁. Right plot: Two UEs, rate region with two channel states ((400, 100) Mbps, and (300, 200) Mbps), with probabilities 0.5. Shown also are the PF throughputs, and the PF-LG-LM throughputs with RG of 120 Mbps for UE₁. We used $a = 0.0005$, $b = 0.000005$.

will be scheduled. However, time-sharing occurs over time, yielding the desired throughputs. In the right plot, the channel has two states, i.e., $\mathcal{S} = \{s', s''\}$; $\bar{\mathcal{R}}$ has the polyhedral shape shown. While the PF-RG-LM algorithm works correctly, our convergence proof does not apply to this case. This remains an item of our current work.

VI. CONCLUSION

Assuming feasibility of the utility optimization problem, we have proposed a slow time-scale update for the additive index-bias that promotes rate guarantees in the usual gradient-type scheduling algorithm. We provide a convergence proof of this algorithm for strictly convex average rate regions. Our simulations show that the slower time-scale index-bias update not only provides accurate maximum utility throughputs, but the index-biases provide very good approximations to the optimum Lagrange multipliers. Practical considerations might require that the throughput averaging time-scale might be specified by the standard or by user requirements, in which case, having a separate time-scale for the index-bias update would be useful for providing a very good estimate of the optimum Lagrange multiplier.

APPENDIX

Global asymptotic stability

We now argue that, for a fixed ν , the o.d.e. (26) has a unique globally asymptotically stable equilibrium. The following proof has been taken from [11], and is provided here for completeness. Recall that (26) is

$$\dot{\theta}(t) = \bar{\mathbf{h}}(\theta(t), \nu) = \arg \max_{r \in \bar{\mathcal{R}}} [\nabla U(\theta(t) + \nu)^T \cdot r - \theta(t)].$$

Let $d(\theta(t), \bar{\mathcal{R}})$ denote the distance of $\theta(t)$ to the set $\bar{\mathcal{R}}$. We first argue that $d(\theta(t), \bar{\mathcal{R}}) \leq d(\theta(0), \bar{\mathcal{R}})e^{-t}$.

Let $\theta_p(t)$ denote the projection of $\theta(t)$ on $\bar{\mathcal{R}}$. Let

$$r(t) = \arg \max_{r \in \bar{\mathcal{R}}} [\nabla U(\theta(t) + \nu)^T \cdot r]$$

Observe that $\theta(t)$ and $r(t)$ are continuous in t , the latter following from Condition 3. For $0 \leq h \leq 1$, $\rho(t+h) := \theta_p(t) + h(r(t) - \theta_p(t)) \in \bar{\mathcal{R}}$, and hence can be used to bound

the distance to $\bar{\mathcal{R}}$ at time $t+h$ for h sufficiently small. We can then upper bound the rate of change of the distance of $\theta(t)$ to the set $\bar{\mathcal{R}}$ as follows:

$$\begin{aligned} & \limsup_{h \downarrow 0} \frac{1}{h} [d(\theta(t+h), \bar{\mathcal{R}}) - d(\theta(t), \bar{\mathcal{R}})] \\ & \leq \limsup_{h \downarrow 0} \frac{1}{h} [\|\theta(t+h) - \theta_p(t+h)\| - \|\theta(t) - \theta_p(t)\|] \\ & = -\|\theta(t) - \theta_p(t)\| \\ & = -d(\theta(t), \bar{\mathcal{R}}) \end{aligned}$$

where the penultimate equality requires an argument that uses the continuity of $\theta(t)$ and $r(t)$ in t .

Thus, for any $\epsilon > 0$ and any bounded set A on the positive orthant, there exists a $T_1 = T_1(\epsilon, A)$ such that $\theta(t) \in \bar{\mathcal{R}}^{(\epsilon)}$ for all $t \geq T_1$, where $\bar{\mathcal{R}}^{(\epsilon)}$ is the ϵ -thickening of $\bar{\mathcal{R}}$, which is the set of all points that are within a distance ϵ of $\bar{\mathcal{R}}$.

We recall Equation 27, which defines $\theta_\infty(\nu)$ as the maximizer of $(U(\theta) + \nu^T \cdot \theta)$ in $\bar{\mathcal{R}}$. Now, fix an arbitrary $\delta > 0$, and denote by $O_\delta(\theta_\infty(\nu))$ the open ball of radius δ around the maximizer. Fix $\epsilon > 0$ small enough so that the maximum of $(U(\theta) + \nu^T \cdot \theta)$ in $(\bar{\mathcal{R}}^{(\epsilon)} \setminus O_\delta(\theta_\infty(\nu))) \cap \mathbb{R}_+^M$, denoted h^* , satisfies $h^* < \max_{\theta \in \bar{\mathcal{R}}} [U(\theta) + \nu^T \cdot \theta]$.

Given that $\theta(0) \in A$, a compact set, the dynamics enters $\bar{\mathcal{R}}^{(\epsilon)}$ and remains there for all $t > T_1(\epsilon, A)$. Further, given that so long as the dynamics remains in $(\bar{\mathcal{R}}^{(\epsilon)} \setminus O_\delta(\theta_\infty(\nu))) \cap \mathbb{R}_+^M$, we have

$$\begin{aligned} & \frac{d}{dt} [U(\theta(t) + \nu^T \cdot \theta(t))] \\ & = [\nabla U(\theta(t) + \nu)^T \cdot (r(t) - \theta(t))] \\ & \geq [\nabla U(\theta(t) + \nu)^T \cdot (\theta_\infty(\nu) - \theta(t))] \\ & \geq (U(\theta_\infty(\nu) + \nu^T \cdot \theta_\infty(\nu)) - ((U(\theta(t) + \nu^T \cdot \theta(t)))) \\ & \geq (U(\theta_\infty(\nu) + \nu^T \cdot \theta_\infty(\nu)) - h^* > 0, \end{aligned}$$

where the second inequality follows from concavity of $(U(\theta) + \nu^T \cdot \theta)$ in θ . This implies that the dynamics must exit $(\bar{\mathcal{R}}^{(\epsilon)} \setminus O_\delta(\theta_\infty(\nu))) \cap \mathbb{R}_+^M$ at some time $t > T_1(\epsilon, A) + T_2$. Combining this with the fact that the dynamics remains in $\bar{\mathcal{R}}^{(\epsilon)}$ for all $t > T_1(\epsilon, A)$, we conclude that $\theta(t) \in O_\delta(\theta_\infty(\nu))$ for all $t \geq T_1(\epsilon, A) + T_2$. Since $\delta > 0$ was arbitrary, we conclude that $\theta(t) \rightarrow \theta_\infty(\nu)$, which establishes the desired global asymptotic stability.

Obtaining ν_{\max} : Two UE Example

To illustrate how it can be determined if there is a bound on the optimum Lagrange multipliers, we provide an illustration for two UEs, UE₀ and UE₁ in which UE₁ has the minimum rate guarantee $\theta_{1,\min}$. By sensitivity analysis of the optimum solution of the optimization problem (1), we can conclude that:

$$\frac{\partial}{\partial \theta_{1,\min}} (U(\theta_0^*(\theta_{1,\min})) + U(\theta_1^*(\theta_{1,\min}))) = -\nu_1^*$$

where $(\theta_0^*(\theta_{1,\min}), \theta_1^*(\theta_{1,\min}))$ is the optimum primal solution, and ν_1^* the optimal dual solution. It follows that

$$U'(\theta_0^*(\theta_{1,\min})) \frac{\partial}{\partial \theta_{1,\min}} \theta_0^*(\theta_{1,\min}) + U'(\theta_1^*(\theta_{1,\min})) \cdot 1 = -\nu_1^*$$

Where, in the second term, we have assumed that $\theta_{1,\min}$ is strictly feasible, i.e., the rate guarantee can be increased. At the point $(\theta_0^*(\theta_{1,\min}), \theta_1^*(\theta_{1,\min}))$ on the boundary of the average rate region $\bar{\mathcal{R}}$ let $(w_0^*, w_1^*) > \mathbf{0}$ be the normal to the boundary. It follows that $\frac{\partial}{\partial \theta_{1,\min}} \theta_0^*(\theta_{1,\min}) = -\frac{w_0^*}{w_1^*} < 0$, which yields

$$v_1^* \leq U'(\theta_0^*(\theta_{1,\min})) \frac{w_0^*}{w_1^*}$$

One way to satisfy Condition 4 is to ensure that the right hand side of the above inequality is bounded.

REFERENCES

- [1] 3GPP. *System Architecture for the 5G System (3GPP TS 23.501 version 15.2.0 Release 15)*, 2018.
- [2] R. Agarwal and V. Subramanian. Optimality of certain channel aware scheduling policies. In *Proc. 40th Annual Allerton Conference on Communications, Control, and Computing*, 2002.
- [3] M. Andrews, S. Mandelli, and S. Borst. Network slicing based on one or more token counters. United States Patent, February 2021. Patent Number US 2021/0037544 A1.
- [4] Albert Banchs, Gustavo de Veciana, Vincenzo Sciancalepore, and Xavier Costa-Perez. Resource allocation for network slicing in mobile networks. *IEEE Access*, 8, 2020.
- [5] M. S. Bazaara, H. D. Sherali, and C. M. Shetty. *Nonlinear Programming: Theory and Algorithms*. John Wiley and Sons, Inc., 1993.
- [6] V. S. Borkar. *Stochastic Approximation: A Dynamical Systems Viewpoint*. Hindustan Book Agency, 2008.
- [7] H. J. Kushner and P. A. Whiting. Convergence of proportional-fair sharing algorithms under general conditions. *IEEE Transactions on Communications*, 3(4), 2004.
- [8] Harold J. Kushner and G. George Yin. *Stochastic Approximation Algorithms and Applications*. Springer, 2003.
- [9] S. Mandelli, M. Andrews, S. Borst, and S. Klein. Satisfying network slicing constraints via 5G MAC scheduling. In *Prof. IEEE Infocom 2019*, April 2019.
- [10] Ravi Kiran Raman and Krishna Jagannathan. Downlink resource allocation under time-varying interference: Fairness and throughput optimality. *IEEE Transactions on Wireless Communications*, 17(2), 2018.
- [11] A. L. Stolyar. On the asymptotic optimality of the gradient scheduling algorithm for multiuser throughput allocation. *Operations Research*, 53(1):12–25, 2005.
- [12] Alexander L. Stolyar. Greedy primal-dual algorithm for dynamic resource allocation in complex networks. *Queueing Systems*, 54, 2006.